

REFINED THEORIES FOR COMPOSITE AND SANDWICH BEAMS WITH C^0 FINITE ELEMENTS

T. KANT† and B. S. MANJUNATH

Department of Civil Engineering, Indian Institute of Technology, Powai, Bombay 400 076, India

(Received 19 October 1988)

Abstract—Refined higher-order displacement models for the behaviour of symmetric and unsymmetric laminated composite beams based on C^0 finite element discretization are presented. These theories incorporate a more realistic non-linear variation of longitudinal displacements through the beam thickness, thus eliminating the use of shear correction coefficient(s). The discrete element considered is a four-noded cubic with kinematic models having three, four and five degrees of freedom per node. The computer program developed incorporates the realistic prediction of interlaminar stresses from equilibrium equations. The present results, when compared with the elasticity solutions, show excellent agreement. In addition numerical results for sandwich beams are presented for future reference.

1. INTRODUCTION

The ever increasing use of composite materials in advanced technology areas, where precision and reliability play a paramount role, demands clear understanding of their behaviour and performance under severe operating environment(s). An understanding of failure due to delamination is of considerable importance. This involves separation of composite laminae especially at the free edge, caused due to low strength along the ply interface and high local interlaminar stresses. Thus, delamination has become a problem of significant concern in the reliable analysis and design of advanced fibre reinforced composite structures. A theory which can predict all these stresses accurately becomes necessary for understanding the failure mechanism of fibre reinforced composite structures.

Structural behaviour of beams may be satisfactorily approximated by the elementary Euler-Bernoulli theory of bending. The main assumption in this theory is that the transverse normal to the reference middle plane remains so during bending, implying that the transverse shear strain becomes zero. Thus, the bending rotation becomes a first derivative of transverse displacement w and hence the theory requires the transverse displacement field to be C^1 continuous. Both compatible and incompatible and complicated higher-order C^1 continuous elements have been derived in the past [1, 2].

The Euler theory may lead to serious discrepancies in the case of deep beams with small aspect ratios where shear effects are significant. Further, the resulting finite element formulation turns out to be computationally inefficient from the point of view of simple finite element procedures. Timoshenko [3] extended the validity of this theory by incorporating the effect of transverse shear strain into the governing equa-

tions. The resulting transverse shear stress distribution was constant through the beam thickness and thus a shear correction coefficient, which is somewhat arbitrary, was introduced to correct the strain energy of deformation. Cowper [4] and Murty [5, 6] have given some new expressions for this coefficient for different cross-sections of the beam, but the discrepancy between the results of this theory and the elasticity solution is seen to be large in the case of built-up beams even after refining the values of shear coefficients.

Stephen and Levinson [7] have given a second order beam theory which is similar to the Timoshenko beam equation but contains two coefficients, one of which depends on cross-sectional warping while the second, although similar in form, includes terms dependent on the transverse direct stresses. Levinson [8-10] has given a fourth order beam theory, which requires two boundary conditions at each end of the beam. Shear correction coefficient(s) is not used as transverse shear deformation is taken into account. Levinson's displacement hypothesis, however, does not adequately describe the two-dimensional displacement pattern.

Rychter [11] has improved the consistency and accuracy of Levinson's theory by embedding in it the two-dimensional linear theory of elasticity and has proved that the corresponding relative mean square error is, in general, proportional to the square of the beam depth. The shear contribution to the error, which comprised of terms multiplied by the shear modulus G , turns out to be proportional to the cube of beam depth. Bickford [12] used Hamilton's principle to derive a consistent higher-order theory of the elastodynamics of the beam based upon the kinematic and stress assumptions previously used by Levinson [8-10].

Thus, recognizing the need for a more refined one-dimensional theoretical model [16], a set of simple higher-order theories are developed here to in-

† To whom correspondence should be addressed.

clude all the secondary effects such as the transverse shear stress, shear strains and their variation across the thickness. Our theoretical models use the C^0 finite elements. The numerical experiments are conducted by using a four-noded cubic element.

2. THEORY AND FORMULATIONS

A set of theoretical models is developed based on the following kinematic assumptions. These are designated as Models 1-4 (see Fig. 1),

Model 1

$$u(x, z) = u_0(x) + z\theta_x(x)$$

$$w(x, z) = w_0(x)$$

Model 2

$$u(x, z) = u_0(x) + z\theta_x(x) + z^2u^*(x)$$

$$w(x, z) = w_0(x)$$

Model 3

$$u(x, z) = u_0(x) + z\theta_x(x) + z^3\theta_x^*(x)$$

$$w(x, z) = w_0(x)$$

Model 4

$$u(x, z) = u_0(x) + z\theta_x(x) + z^2u^*(x) + z^3\theta_x^*(x)$$

$$w(x, z) = w_0(x)$$

where the parameters u and w define the displacement components in the coordinate directions x and z respectively at any point in the beam domain. Here we present all the derivations only for Model 4 given in eqn (4). Other theoretical models become special cases of Model 4. The variations in the cases of Models 1-3 are given concisely in Appendix A. The following relations are obtained by substituting eqn (4) into strain displacement relations of three-dimensional elasticity [13],

$$\epsilon_x = \epsilon_{x0} + z\kappa_x + z^2\epsilon_{x0}^* + z^3\kappa_x^*$$

$$\epsilon_z = 0$$

$$\gamma_{xz} = \phi + z\kappa_{xz} + z^2\phi^* \tag{5}$$

where

$$[\epsilon_{x0}, \kappa_x, \epsilon_{x0}^*, \kappa_x^*] = \left[\frac{\partial u}{\partial x}, \frac{\partial \theta_x}{\partial x}, \frac{\partial u^*}{\partial x}, \frac{\partial \theta_x^*}{\partial x} \right]$$

$$[\phi, \kappa_{xz}, \phi^*] = \left[\theta_x + \frac{\partial u}{\partial x}, 2u^*, 3\theta_x^* \right] \tag{6}$$

In truth, each lamina in the laminate is in a two-dimensional stress state. However, the transverse normal stress is usually negligibly small. The constitute relation for a typical lamina L is thus written simply as [17],

$$\begin{bmatrix} \sigma_x \\ \tau_{xz} \end{bmatrix} = \begin{bmatrix} E & 0 \\ 0 & G \end{bmatrix} \begin{bmatrix} \epsilon_x \\ \gamma_{xz} \end{bmatrix} \tag{7}$$

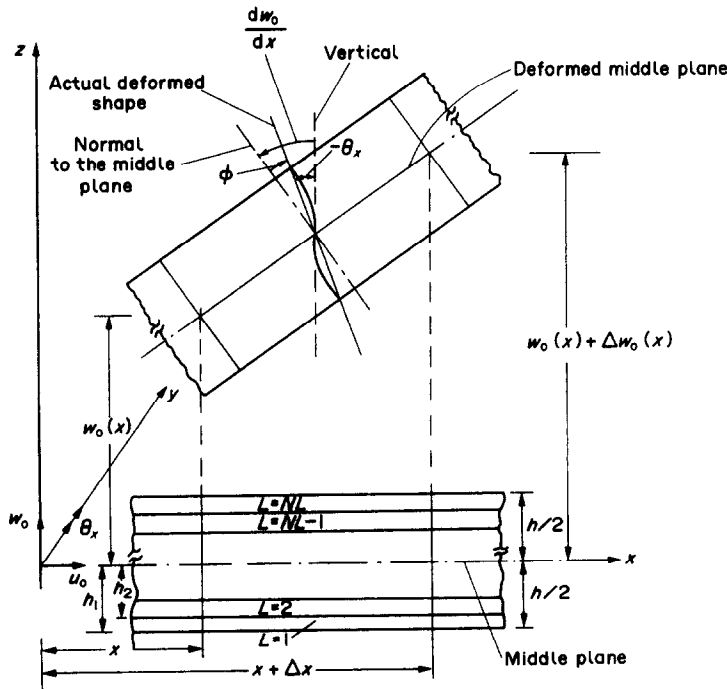


Fig. 1. Laminate geometry with positive set of lamina/laminate reference axes and displacement components.

where σ_x, τ_{xz} are the stresses and ϵ_x, γ_{xz} are the strain components referred to the lamina coordinates $(x-z)$.

The total potential energy Π of a beam of width b can be written as,

$$\Pi = \frac{b}{2} \int_z \int_1 \epsilon' \sigma \, dx \, dz - b \int_z \int_1 (\mathbf{u})' \mathbf{p} \, dx \, dz, \quad (8)$$

where

$$\begin{aligned} \epsilon &= [\epsilon_x, \gamma_{xz}]' & \sigma &= [\sigma_x, \tau_{xz}]' \\ u &= [u, w]' & \mathbf{p} &= [p_x, p_z]'. \end{aligned} \quad (9)$$

The superscript t denotes the transpose of a vector/matrix. The expressions for the strain components given by eqn (5) are substituted in eqn (8). The following relations result when an explicit integration is carried out through the beam thickness,

$$\begin{aligned} \Pi &= \frac{b}{2} \int_1 [\epsilon_{x0} N_x + \kappa_x M_x + \epsilon_{x0}^* N_x^* + \kappa_x^* M_x^*] \, dx \\ &+ \frac{b}{2} \int_1 [\phi Q + \kappa_{xz} S + \phi^* Q^*] \, dx - b \int_1 (\delta)' \mathbf{p}_0 \, dx \end{aligned} \quad (10)$$

or in a compact form,

$$\Pi = \frac{b}{2} \int_1 \bar{\epsilon}' \bar{\sigma} \, dx - b \int_1 (\delta)' \mathbf{p}_0 \, dx, \quad (11)$$

in which

$$\begin{aligned} \bar{\sigma} &= [N_x, N_x^*, M_x, M_x^*, Q, Q^*, S]' \\ \bar{\epsilon} &= [\epsilon_{x0}, \epsilon_{x0}^*, \kappa_x, \kappa_x^*, \phi, \phi^*, \kappa_{xz}]' \\ \delta &= (u_0, w_0, \theta_x, u_0^*, \theta_x^*)' \\ \mathbf{p}_0 &= (p_{x0}, p_{z0}, m_{x0}, p_{x0}^*, m_{x0}^*)'. \end{aligned} \quad (12)$$

The stress-resultants in eqn (10) above are defined as follows:

$$\begin{aligned} \begin{bmatrix} N_x & M_x & N_x^* & M_x^* \\ Q_x & S & Q_x^* & 0 \end{bmatrix} &= \\ \sum_{L=1}^{NL} \int_{h_L}^{h_{L+1}} \begin{bmatrix} \sigma_x \\ \tau_{xz} \end{bmatrix} [1, z, z^2, z^3] \, dz. \end{aligned} \quad (13)$$

Upon integration, these are written in matrix form as follows:

$$\begin{bmatrix} \mathbf{N} \\ \mathbf{M} \\ \mathbf{Q} \end{bmatrix} = \begin{bmatrix} \mathbf{D}_M & \mathbf{D}_c & 0 \\ \mathbf{D}_c' & \mathbf{D}_B & 0 \\ 0 & 0 & \mathbf{D}_s \end{bmatrix} \begin{bmatrix} \epsilon \\ \kappa \\ \phi \end{bmatrix} \quad (14)$$

or,

$$\bar{\sigma} = \mathbf{D} \bar{\epsilon} \quad (15)$$

where

$$\begin{aligned} \mathbf{N} &= (N_x, N_x^*)' & \mathbf{M} &= (M_x, M_x^*)' \\ \mathbf{Q} &= (Q_x, Q_x^*, S)' & \epsilon &= (\epsilon_{x0}, \epsilon_{x0}^*)' \\ \kappa &= (\kappa_x, \kappa_x^*)' & \phi &= (\phi_x, \phi_x^*, \kappa_{xz})' \end{aligned} \quad (16)$$

$$\mathbf{D}_M = \sum_{L=1}^{NL} \begin{bmatrix} Eh_1 & Eh_3 \\ Eh_3 & Eh_5 \end{bmatrix} \quad (17)$$

$$\mathbf{D}_s = \sum_{L=1}^{NL} \begin{bmatrix} Gh_1 & Gh_3 & Gh_2 \\ & Gh_5 & Gh_4 \\ \text{symm.} & & Gh_3 \end{bmatrix} \quad (18)$$

$$h_i = 1/i(h_{L+1}^i - h_L^i) \quad i = 1, 2, \dots, 7. \quad (19)$$

The coefficients of the \mathbf{D}_c matrix can be obtained by replacing h_1, h_3, h_5 by h_2, h_4, h_6 respectively in the \mathbf{D}_M matrix. Similarly the coefficients of the \mathbf{D}_B matrix can be obtained by replacing h_1, h_3, h_5 by h_3, h_5, h_7 respectively in the \mathbf{D}_M matrix.

The interlaminar transverse stresses (τ_{xz}, σ_z) cannot be accurately estimated by eqn (7). This is mainly due to the fact that the constitutive laws are discontinuous, whereas interlaminar stresses have to maintain continuity across the interfaces. The three/two-dimensional analysis becomes very complex due to thickness variation of constitutive laws and continuity requirements across the interfaces. Even finite element schemes cannot be applied by using three/two-dimensional displacement-based elements, as a large number of elements are required to gain acceptable levels of accuracy particularly with reference to stress continuity requirements at the interface, because here again, one has to depend on the constitutive relations. For these reasons, the interlaminar stresses between the layers L and $L+1$ at z are obtained by integrating the two equilibrium equations of two-dimensional elasticity for each layer over the lamina thickness and summing over layer 1 to L as follows.

The equations of equilibrium representing the pointwise equilibrium can be written as

$$\tau_{,j} = 0 \quad i, j = x, z. \quad (20)$$

Substituting the lamina stress in eqn (20) and integrating, the interlaminar shear stress can be obtained as,

$$\tau_{xz}^L|_{z=h_{L+1}} = - \sum_{i=1}^L \int_{h_i}^{h_{i+1}} \frac{\partial \sigma_x}{\partial x} \, dz + C_1. \quad (21)$$

Substituting the lamina stress in eqn (20) and eliminating interlaminar shear stress, the following second order differential equation is obtained,

$$\frac{\partial^2 \sigma_z}{\partial z^2} = \frac{\partial^2 \sigma_x}{\partial x^2}. \quad (22)$$

The following equation is obtained for interlaminar normal stress after integrating eqn (22) twice,

$$\sigma_z^L|_{z=h_{L+1}} = \sum_{i=1}^L \int_{h_i}^{h_{i+1}} \left(\int_z \frac{\partial^2 \sigma_x}{\partial x^2} dz \right) dz + zC_2 + C_3. \quad (23)$$

Thus, it is seen that by choosing stress equilibrium equations, estimates of interlaminar stresses can be obtained. For estimates of in-plane stresses and strains, displacement-based finite element models can be used. Stresses in laminates can be evaluated in this manner, but in interlaminar shear stress [eqn (21)], it may be noted that in view of the availability of only a single constant of integration, the interlaminar shear stress estimate may not in general satisfy beam boundary conditions at the boundary surfaces $z = \pm h/2$.

In the case of interlaminar normal stress, this problem does not arise, as here two constants of integration obtained by integrating twice can be determined by substituting two boundary conditions at $z = \pm h/2$. Equation (21) is substituted in a second equilibrium equation given by eqn (20) to get the continuity of σ_z across the thickness. Equation (23) is solved as a boundary value problem instead of an initial value problem as in eqn (21), but this requires use of at least a cubic element, so that the third derivatives of displacements can be determined. Thus, in all these theories four-noded cubic elements are used in the numerical study.

3. FINITE ELEMENT FORMULATION

In the standard finite element technique, the total solution domain is discretized into NE subdomains (elements), such that

$$\Pi(\delta) = \sum_{e=1}^{NE} \Pi^e(\delta), \quad (24)$$

where Π and Π^e are the total potential energies of the system and the element respectively. The potential energy for an element e can be expressed in terms of internal strain energy U^e and the external work done W^e , such that

$$\Pi^e(\delta) = U^e - W^e, \quad (25)$$

in which δ is the vector of unknown displacement variables in the problem, defined in eqn (12). In C^0 finite element theory, the continuum displacement vector within the element is discretized such that

$$\delta = \sum_{i=1}^{NN} N_i \delta_i, \quad (26)$$

where NN is the number of nodes in an element, N_i is the interpolating function associated with node i

and δ_i is the generalized displacement vector corresponding to the i th node of an element.

Knowing the generalized displacement vector δ at all points within the element, the generalized strain at any point given by eqn (6) can be expressed in matrix form as follows [14]:

$$\bar{\epsilon} = \sum_{i=1}^{N_A} \mathbf{B}_i \delta_i, \quad (27)$$

where

$$\bar{\epsilon} = (\epsilon_{x0}, \epsilon_{x0}^*, \kappa_x, \kappa_x^*, \phi, \phi^*, \kappa_{xz})'. \quad (28)$$

The \mathbf{B}_i matrix has a dimension of 7×5 , in which the non-zero elements are

$$B_{1,1} = B_{2,4} = B_{3,3} = B_{4,5} = B_{5,2} = \frac{\partial N_i}{\partial x}$$

$$B_{5,3} = N_i, \quad B_{6,5} = 3N_i, \quad B_{7,4} = 2N_i. \quad (29)$$

Upon evaluating the \mathbf{D} and \mathbf{B}_i matrices as given by eqns (15) and (29) respectively, the element stiffness matrix can be computed by using the standard relation [14]:

$$\mathbf{K}_e^c = b \int_{-1}^{+1} \mathbf{B}_i^T \mathbf{D} \mathbf{B}_i |\mathbf{J}| d\xi. \quad (30)$$

The computation of the element stiffness matrix \mathbf{K}^e is economized by explicit multiplication of \mathbf{B}_i , \mathbf{D} and \mathbf{B}_i matrices instead of carrying out the full matrix multiplication of the triple product. In addition, due to the symmetry of the stiffness matrix, only the blocks \mathbf{K}_{ij} lying on one side of the main diagonal are formed. The integral is evaluated by a selective integration technique with four and three Gauss quadrature rules for membrane-flexure and shear parts respectively as follows:

$$\mathbf{K}_{ij}^c = b \sum_{a=1}^g W_a \mathbf{B}_i^T \mathbf{D} \mathbf{B}_j |\mathbf{J}| d\xi, \quad (31)$$

where W_a is the weighting coefficient, g is the number of numerical quadrature points and $|\mathbf{J}|$ is the Jacobian conversion.

The consistent load vector \mathbf{p}_i due to uniformly distributed transverse load q can be written as

$$\mathbf{p}_i = \int_{-1}^{+1} N_i^T q |\mathbf{J}| d\xi. \quad (32)$$

The integral of eqn (32) is evaluated numerically using the four Gauss quadrature rule. The result is

$$\mathbf{p}_i = \sum_{a=1}^g W_a N_i^T(0, q, 0, 0, 0) |\mathbf{J}| d\xi. \quad (33)$$

The consistent load vector for sinusoidal transverse

load can be obtained by using the following substitution in expression (33),

$$q = q_0 \sin\left(\frac{m\pi x}{l}\right), \quad (34)$$

where l is the beam dimension, x is the Gauss point coordinate and m is the usual harmonic number.

4. NUMERICAL RESULTS AND DISCUSSION

In the present study a four-noded Lagrangian cubic isoparametric element with varying degrees of freedom per node is employed. All the computations were carried out on a CYBER 180/840 computer in single precision with 16 significant digits as word length. In order to compare the results with the elasticity solution and CPT given by Pagano [15],

layers of unidirectional fibrous composite materials possessing the following stiffness properties, which simulate a high modulus graphite/epoxy composite, have been considered

$$E_L = 25 \times 10^6 \quad E_T = 1 \times 10^6$$

$$G_{LT} = 0.50 \times 10^6 \quad \nu = 0.25,$$

where L signifies the direction parallel to the fibres, T is the transverse direction and ν is Poisson's ratio measuring strain in the transverse direction under uniaxial normal stress in the L direction.

Three separate geometrical configurations are considered, namely

- (1) A unidirectional beam with the fibres oriented in the X -direction.

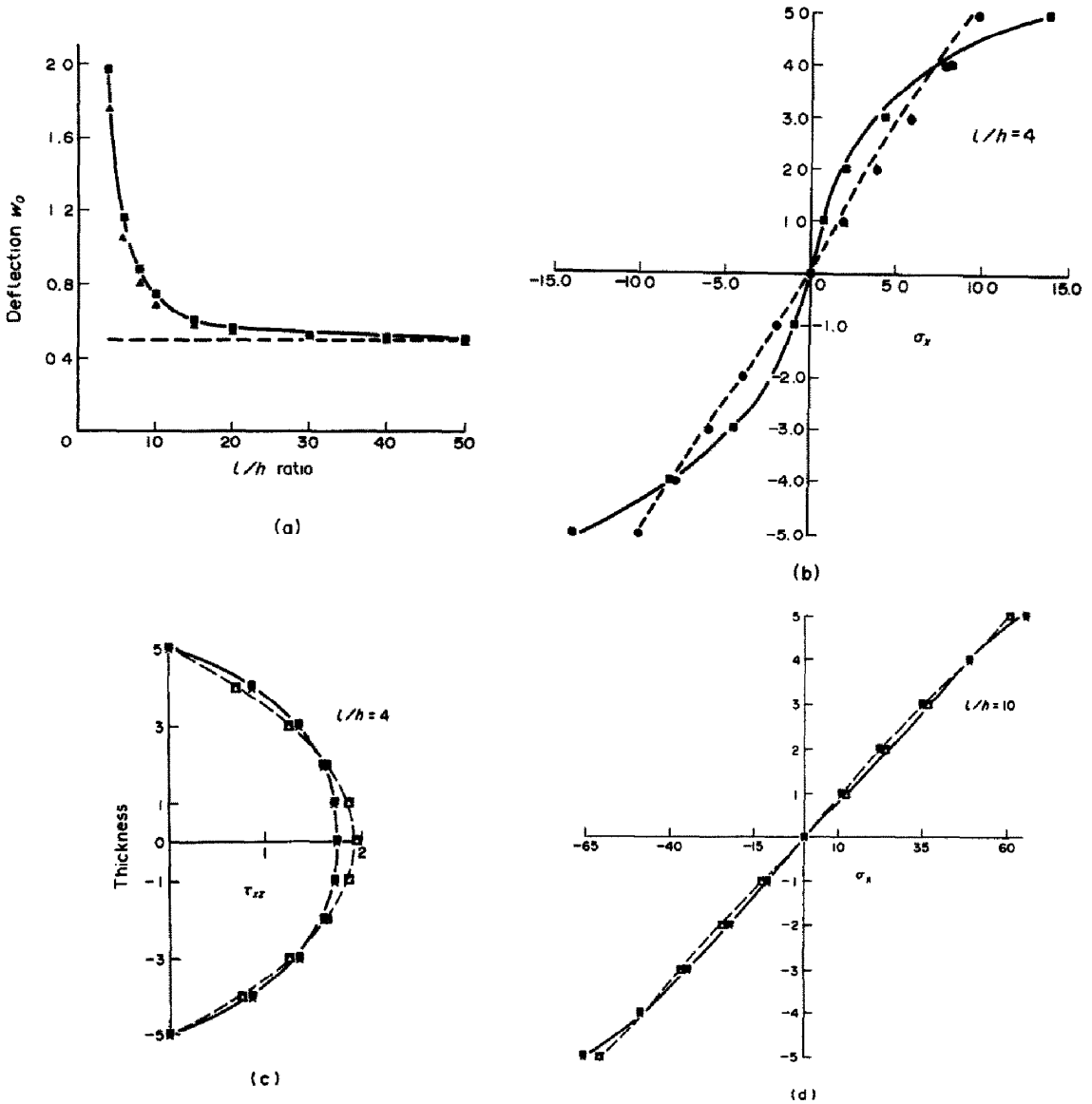


Fig. 2. (a) Deflection w_0 vs l/h ratio. (b) Thickness vs in-plane stress. (c) Thickness vs interlaminar shear stress. (d) Thickness vs in-plane stress.

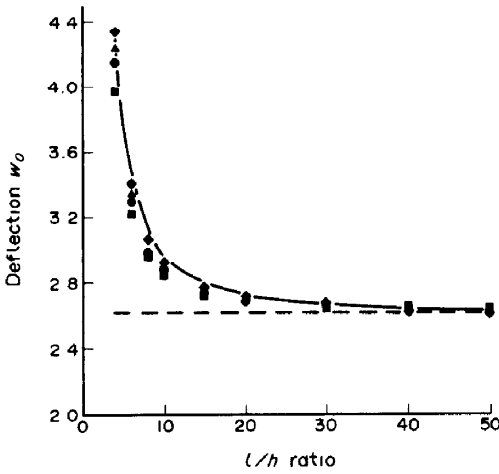
- (2) A bidirectional (coupled) laminate with the T and L directions aligned parallel to x in the top and bottom layers respectively, the layers being of equal thickness.
- (3) A symmetric three-ply laminate with layers of equal thickness, the L layer coinciding with x in the outer layers, while T is parallel to x in the central layer.

In these problems sinusoidal loading is considered. A shear correction coefficient of 1.2 is used for Model 1, since it does not contain the higher-order terms. The following non-dimensionalized quantities are used in connection with Figs 2-5,

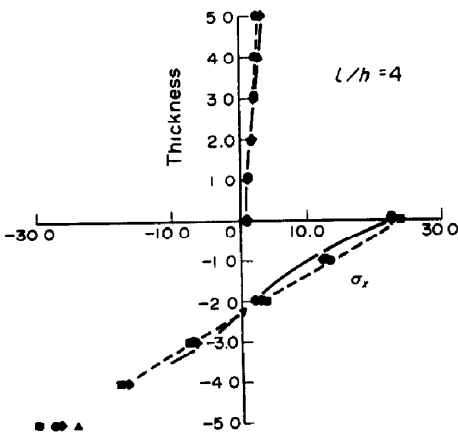
$$\bar{\sigma}_x = \frac{\sigma_x(l/2, z)}{q_0}, \quad \bar{\sigma}_z = \frac{\sigma_z(l/2, z)}{q_0}, \quad \bar{\tau}_{xz} = \frac{\tau_{xz}(0, z)}{q_0}$$

$$\bar{u} = \frac{E_T u(0, z)}{hq_0}, \quad \bar{w} = \frac{100E_T h^3 w_0(l/2, 0)}{q_0 l^4} \quad (35)$$

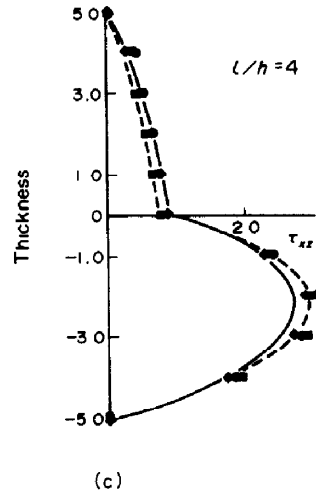
The relationship of the maximum deflection w_0 and l/h ratio is shown for the three configurations in Figs



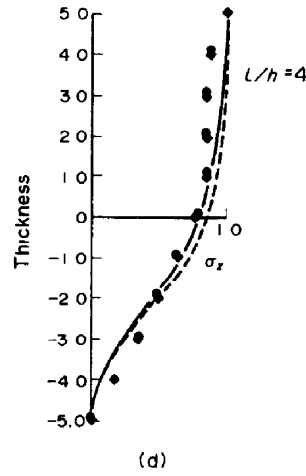
(a)



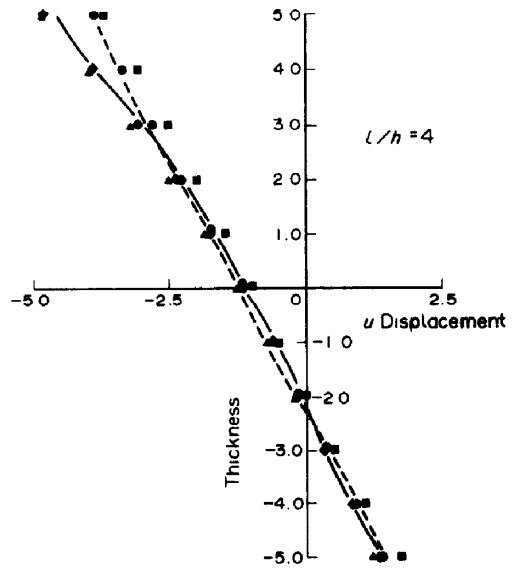
(b)



(c)

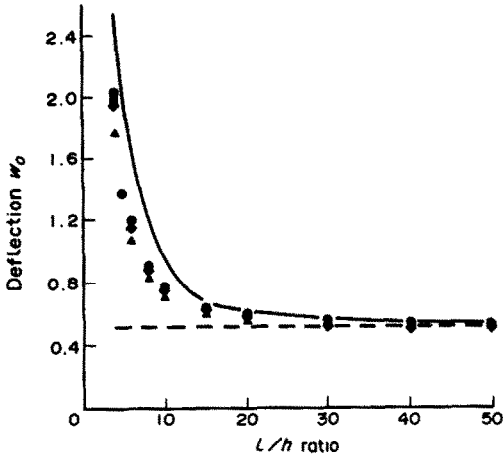


(d)

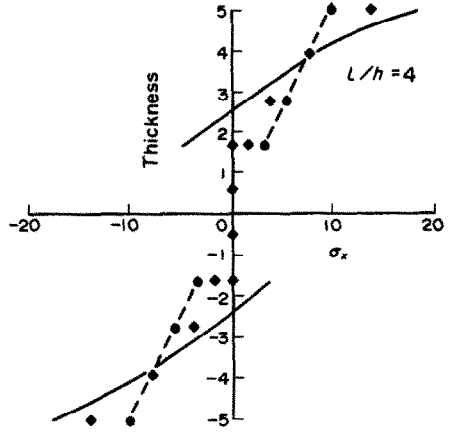


(e)

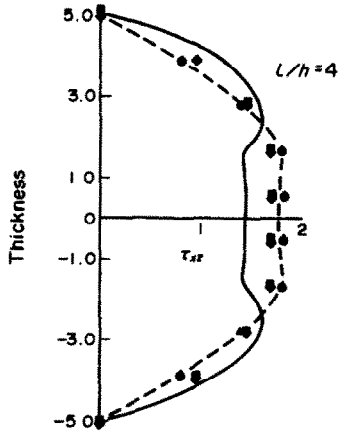
Fig. 3. (a) Deflection w_0 vs l/h ratio. (b) Thickness vs in-plane stress. (c) Thickness vs interlaminar shear stress. (d) Thickness vs interlaminar normal stress. (e) Thickness vs u displacement.



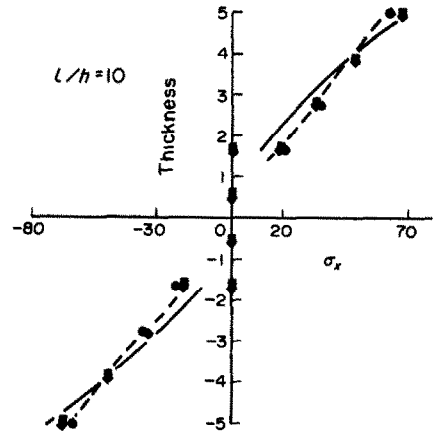
(a)



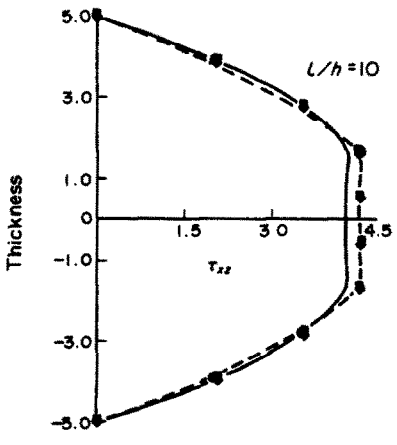
(b)



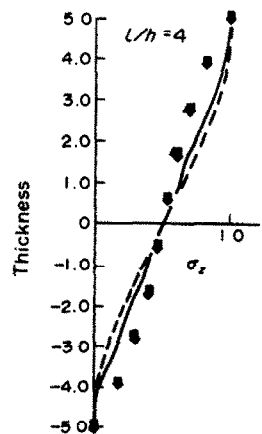
(c)



(d)



(e)



(f)

Fig. 4. a-f

continued over

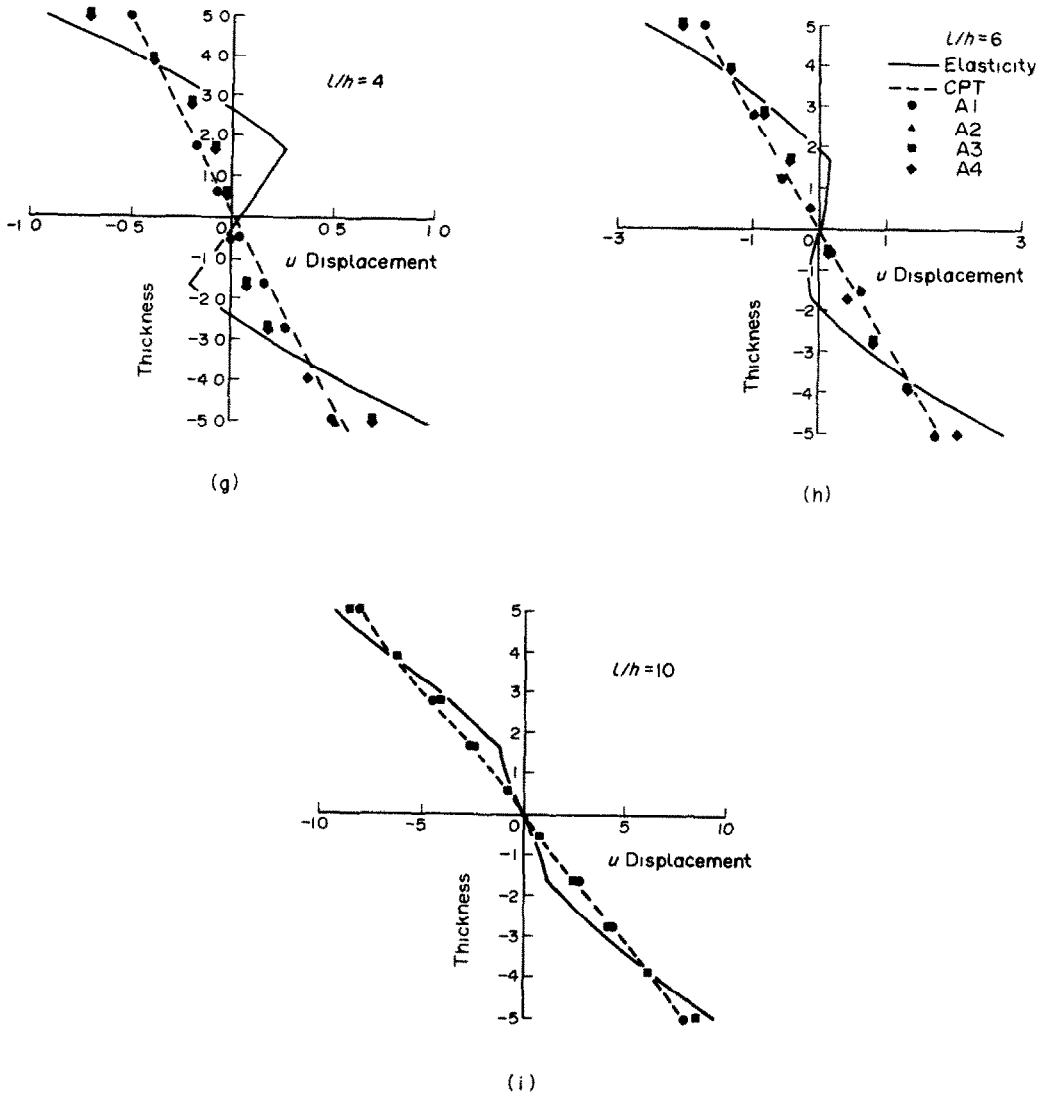


Fig. 4. (a) Deflection w_0 vs l/h ratio. (b) Thickness vs in-plane stress. (c) Thickness vs interlaminar shear stress. (d) Thickness vs in-plane stress. (e) Thickness vs interlaminar shear stress. (f) Thickness vs interlaminar normal stress. (g) Thickness vs u displacement. (h) Thickness vs u displacement. (i) Thickness vs u displacement.

2a, 3a and 4a. The present theory slightly underestimates the displacement compared to the elasticity solution for lower values of l/h , but from $l/h = 20$ both theories give the same values. The CPT underestimates the deflections and gives a very poor estimate for relatively low values of l/h .

The in-plane stress σ_x distribution is shown in Figs 2b, 3b and 4b for $l/h = 4$. Models 3 and 4 estimate values very close to the elasticity solution compared to Models 1 and 2 in all cases. Figures 2d and 4d show the distribution of σ_x for case 1 and case 3 for $l/h = 10$. In case 3 some differences in results are obtained at the interfaces of the laminates. After that the results closely follow the elasticity solution as it reaches the top/bottom surfaces in the cases of Models 3 and 4.

Table 1. Displacement and stresses for sandwich beams

Models	l/h	$w_0/10$	$\sigma_x/10^3$	τ_{xz}^0
1	4	1.265838	0.07142	1.351
2		1.202870	0.07138	1.350
3		3.946953	0.07683	1.341
4		3.963281	0.07672	1.343
TIMO		1.265356	0.06982	1.320
1	10	0.946352	0.4463	3.376
2		0.946278	0.4463	3.376
3		1.377320	0.4518	3.369
4		1.380100	0.4515	3.369
TIMO		0.945870	0.4363	3.299
1	50	0.887952	11.16	16.88
2		0.887540	11.16	16.88
3		0.905208	11.16	16.88
4		0.905320	11.16	16.88
TIMO		0.887474	10.19	16.49

The distribution of τ_{xz} is shown in Figs 2c, 3c and 4c for $l/h = 4$. Only in case 3 were significant differences in results obtained. Hence in Fig. 4e the distribution for $l/h = 10$ is shown. In this case the present theory follows the elasticity theory in the outer layers, but in the middle layers it is close to the CPT theory. The distribution of σ_z for cases 2 and 3 is shown in Figs 3d and 4f for $l/h = 4$. The difference between results is greater in case 3 and it slightly underestimates the value compared to the elasticity solution near the top surface of the beam.

A simply supported sandwich beam under sinusoidal loading is considered next for comparison of displacement and stresses. The following material properties are used [18],

Stiff layers:

$$E_1 = E_2 = 10^7 \quad G = E_1/(1 + \nu) \quad \nu = 0.30$$

$$\frac{h_{\text{core1}}}{h_{\text{stiff}}} = \frac{h_{\text{core2}}}{h_{\text{stiff}}} = 20.$$

Core below the midplane:

$$G = 5 \times 10^3 \quad \nu = 0 \quad E = 2G.$$

Core above the midplane:

$$G = 3 \times 10^4 \quad \nu = 0 \quad E = 2G.$$

The results for displacement, in-plane stress and τ_{xz} for different l/h ratios are shown in Table 1. The variation of in-plane displacement u , τ_{xz} and σ_z are shown in Fig. 5a–c. The results show large variations of displacements and stresses for Models 3 and 4 for thick beams ($l/h = 4$) compared to Timoshenko's theory, Models 1 and 2. The values are almost equal to the latter for thin beams ($l/h = 50$).

5. CONCLUSIONS

The results from a set of higher-order theories (Models 2, 3 and 4) for simply supported composite and sandwich beams subjected to sinusoidal loading are presented. These theories do not require the usual shear correction coefficient(s) (Model 1, which is Timoshenko's theory). The results show excellent agreement with the elasticity solution for thick-to-thin beams. In the case of sandwich beams, large differences in results were obtained compared to Timoshenko's theory, which uses an arbitrary shear correction coefficient with a linear longitudinal displacement variation through the beam thickness. While here the discussion is limited to a particular type of loading and boundary conditions, these theories can be used to tackle any type of loading and boundary conditions. Our emphasis here was to establish the credibility of our formulations to predict, especially, the transverse interlaminar stresses

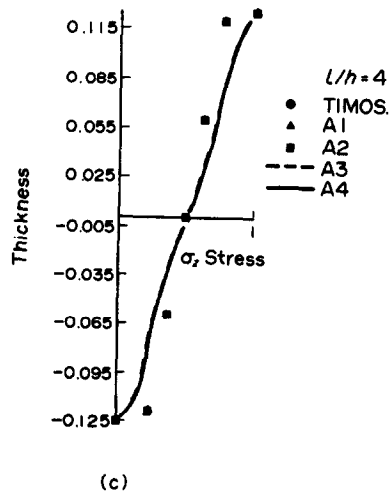
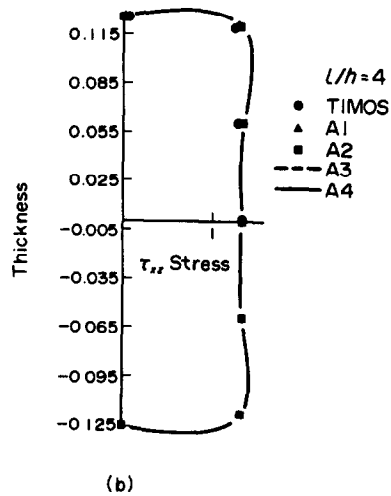
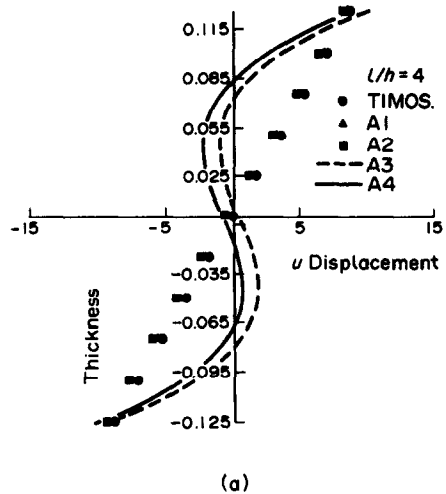


Fig. 5. (a) Thickness vs u displacement. (b) Thickness vs interlaminar shear stress. (c) Thickness vs interlaminar normal stress.

(σ_z and τ_{xz}). For this reason, we limited ourselves to problems for which exact elasticity solutions were available. The numerical estimate of these transverse stresses, which is of paramount importance in the design of laminates, is not available to date. This is due to the numerical problem of higher-order numerical differentiation in the longitudinal direction associated with the integration of the elasticity equilibrium equations. The use of cubic C^0 elements seems to have given fairly accurate estimates of these stresses.

In the symmetric case, the results of Models 1 and 3 agree closely with the results of Models 2 and 4 respectively, as the in-plane displacements are negligible due to the transverse loading pattern. Thus, for symmetric composites and sandwich beams under transverse loads, Model 3 can be used to calculate the displacements and stresses as these values are close to the elasticity solution.

In the unsymmetric case, the results of Model 4 are closest to the elasticity solution compared with the other models. Thus, this model can be used to tackle unsymmetric composites and sandwich beams.

Acknowledgement—Partial support of this research by the Aeronautics Research and Development Board, Ministry of Defence, Government of India through its Grants Aero/RD-134/100/84-85/362 and Aero/RD-134/100/10/88-89/518 is gratefully acknowledged

REFERENCES

1. G. P. Bazeley, Y. K. Cheung, B. M. Irons and O. C. Zienkiewicz, Triangular elements in bending conforming and nonconforming solutions. *Proc. 1st Conf. on Matrix Methods in Structural Mechanics*, AFFDL-TR-60-80, 547-576, OH (1965).
2. I. Holland and K. Bell, *Finite Element Methods in Stress Analysis*. Tech. Univ. of Norway, Tapir (1969).
3. S. P. Timoshenko, On the correction for shear in differential equations for transverse vibrations of prismatic bars. *Phil. Mag., Ser. 641*, 744-746 (1921).
4. G. R. Cowper, The shear co-efficient in Timoshenko beam theory. *ASME J. appl. Mech.* **33**, 335-340 (1966).
5. A. V. K. Murty, Vibration of short beams. *AIAA Jnl* **8**, 34-38 (1970).
6. A. V. K. Murty, Analysis of short beams. *AIAA Jnl* **8**, 2098-2100 (1970).
7. N. G. Stephen and M. Levinson, A second order beam theory. *J. Sound Vibr.* **67**, 293-305 (1979).
8. M. Levinson, A new rectangular beam theory. *J. Sound Vibr.* **74**, 81-87 (1981).
9. M. Levinson, On Bickford's consistent higher-order beam theory. *Mech. Res. Commun.* **12**, 1-9 (1985).
10. M. Levinson, Further results of a new beam theory *J. Sound Vibr.* **77**, 440-444 (1981).
11. Z. Rychter, On the accuracy of a beam theory. *Mech. Res. Commun.* **14**, 99-105 (1987).
12. W. B. Bickford, A consistent higher-order beam theory. *Devl theor. appl. Mech.* **11**, 137 (1982).
13. S. P. Timoshenko and J. N. Goodier, *Theory of Elasticity*. McGraw-Hill, Singapore (1985).
14. O. C. Zienkiewicz, *The Finite Element Method* McGraw-Hill, London (1977).

15. N. J. Pagano, Exact solution for composite laminates in cylindrical bending. *J. Compos. Mater.* **3**, 398-410 (1969).
16. T. Kant and A. Gupta, A finite element model for a higher-order shear-deformable beam theory. *J. Sound Vibr* **125**, 193-202 (1988).
17. R. M. Jones, *Mechanics of Composite Materials*. McGraw-Hill, Kagakusha, Tokyo (1975).
18. B. N. Pandya, Higher-order theories and finite element evaluations for multilayered composite plates. Ph.D Thesis, Department of Civil Engineering, IIT, Bombay (1987).

APPENDIX A

Model 1.

$$\delta = (u_0, w_0, \theta,)' \tag{A1}$$

The membrane-flexure and coupling matrix can be obtained by replacing h_3, h_5 by h_2, h_4 respectively in eqn (17). The D_s matrix has a dimension of (1×1) which is equal to the first term in eqn (18).

The non-zero elements of the $B_s(3 \times 3)$ matrix can be written as follows,

$$B_{1,1} = B_{2,3} = B_{3,2} = \frac{\partial N_1}{\partial x}, \quad B_{3,3} = N_1. \tag{A2}$$

Model 2:

$$\delta = (u_0, w_0, \theta, u_0^*)'. \tag{A3}$$

The membrane-flexure and coupling matrix can be written as follows,

$$\sum_{L=1}^{NL} \begin{bmatrix} Eh_1 & Eh_2 & Eh_3 \\ & Eh_3 & Eh_4 \\ \text{symm.} & & Eh_5 \end{bmatrix}. \tag{A4}$$

The D_s matrix can be obtained by replacing h_3, h_5 by h_2, h_4 respectively in the first (2×2) matrix of eqn (18).

The non-zero elements of the $B_s(5 \times 4)$ can be written as follows,

$$B_{1,1} = B_{2,3} = B_{3,4} = B_{4,2} = \frac{\partial N_1}{\partial x}$$

$$B_{4,3} = N_1, \quad B_{5,4} = 2N_1. \tag{A5}$$

Model 3:

$$\delta = (u_0, w_0, \theta, \theta^*)'. \tag{A6}$$

The membrane-flexure and coupling matrix can be written as follows,

$$\sum_{L=1}^{NL} \begin{bmatrix} Eh_1 & Eh_2 & Eh_4 \\ & Eh_3 & Eh_5 \\ \text{symm.} & & Eh_7 \end{bmatrix}. \tag{A7}$$

The D_s matrix is equal to the first (2×2) matrix of eqn (18).

The non-zero elements of the $B_s(5 \times 4)$ matrix can be written as follows,

$$B_{1,1} = B_{2,3} = B_{3,4} = B_{4,2} = \frac{\partial N_1}{\partial x}$$

$$B_{4,3} = N_1, \quad B_{5,4} = 3N_1. \tag{A8}$$